Steady State Creep Behavior of Functionally Graded Thick Cylinder

Tejeet Singh, Harmanjit Singh

Abstract—Creep behavior of thick-walled functionally graded cylinder consisting of AlSiC and subjected to internal pressure and high temperature has been analyzed. The functional relationship between strain rate with stress can be described by the well known threshold stress based creep law with a stress exponent of five. The effect of imposing non-linear particle gradient on the distribution of creep stresses in the thick-walled functionally graded composite cylinder has been investigated. The study revealed that for the assumed non-linear particle distribution, the radial stress decreases throughout the cylinder, whereas the tangential, axial and effective stresses have averaging effect. The strain rates in the functionally graded composite cylinder could be reduced to significant extent by employing non-linear gradient in the distribution of reinforcement.

Keywords—Functionally Graded Material, Pressure, Steady State Creep, Thick-Cylinder.

I. INTRODUCTION

CLINDER shave been receiving considerable importance due to their large scale structural and industrial applications. In many of these applications like transportation of high pressurized fluids and nuclear reactors pipes, it has to work under high mechanical and thermal loading conditions. As a result, the cylinder undergoes considerable creep deformations, and reducing the service lifetime. The experimental testing and estimation of creep deformations in functionally graded materials (FGMs) are quite complicated, time consuming and costly affair. Therefore, from practical point of view, the prediction of creep deformations for determining the service lifetime of structural components made of FGMs is of great importance. Functionally graded materials are the advanced composite where the reinforcement content is smoothly varied in some direction to achieve desired variation in the material properties. FGMs have been developed as ultra high temperature resistant materials for potential applications in aircrafts, space vehicles and other structural components exposed to elevated temperature [1]. In recent years, the problem of creep in cylinders made of FGMs and operating under high pressure and temperature has attracted the interest of many researchers. Fukui and Yamanaka [2] investigated the effects of the gradation of components on the strength and deformation of thick-walled FG tubes under internal pressure. Chen et al. [3] studied the creep behavior of thick-walled cylinders made of FGM and subjected to both internal and external pressures. They obtained the asymptotic solutions on the basis of a Taylor expansion series and compared it with the results of Finite Element analysis (FEA) obtained by using ABAQUS software. You et al. [4] analyzed the steady state creep in thick walled cylinders made of arbitrary FGMs and subjected to internal pressure. The impact of radial variations of material parameters on the stresses in the cylinder was investigated. Abrinia et al. [5] obtained analytical solution for computing the radial and circumferential stresses in a thick FG cylindrical vessel under the influence of internal pressure and temperature. In the light of this, it is decided to investigate steady state creep in a thick-walled FG cylinder consisting of silicon carbide particles (SiCp) embedded in Aluminum (Al) matrix and subjected to internal pressure.

II. DISTRIBUTION OF REINFORCEMENT

In the thick-walled functionally graded cylinder, the SiCp are assumed to vary non-linearly from the inner radius a to the outer radius b. The reinforcement content *(vol %)* of silicon carbide $V(r)$ at any radius r is assumed to vary according to the following equation,

$$V(r) = V_{max} - \left(\frac{r-a}{b-a}\right)^2 \left[V_{max} - V_{min}\right] \qquad (1)$$

where, V_{max} and V_{min} are the maximum and minimum reinforcement content respectively at the inner and the outer radius. The average particle content (V_{avg}) in the cylinder of length 'l' can be expressed as,

$$V_{avg} = \frac{\int_a^b 2\pi r V(r)dr}{\pi(b-a)^2 l} \qquad (2)$$

Putting the value of $V(r)$ from (1) into (2) and integrating, we get,

$$V_{min} = \frac{3V_{avg}(1-\psi^2)(1-\psi) - V_{max}(1-3\psi^2 + 2\psi^3)}{(2-3\psi+\psi^3)} \qquad (3)$$

where ψ is the ratio of inner radius (a) and outer radius (b).

III. CREEP LAW AND CREEP PARAMETERS

For aluminum matrix composites (AMCs), undergoing steady state creep, the functional relation between effective

T. Singh is with the Shahhed Bhagat Singh State State Technical Campus, Ferozepur, Punjab, India (phone: +918288012011; fax: 01632242138; e-mail: tejeetsingh@rediffmail.com).

H. Singh was with Amritsar College of Engineering and Technology, Amritsar, Punjab, India.

strain rate $(\dot{\varepsilon}_e)$ with effective stress (σ_e) can be described by the well known threshold stress [6] based creep law,

$$\dot{\varepsilon}_e = A'\left(\frac{\sigma_e - \sigma_0}{E}\right)^n \exp\left(\frac{-Q}{RT}\right) \tag{4}$$

where A', n, Q, E, R and T denotes respectively the structure dependent parameter, true stress exponent, true activation energy, temperature-dependent Young modules, gas constant and operating temperature. The creep law given by (4) may alternatively be written as;

$$\dot{\varepsilon}_e = \left[M(r)(\sigma_e - \sigma_o(r)\right]^n \tag{5}$$

where, $M = \frac{1}{E}\left(A' \exp\frac{-Q}{RT}\right)^{1/n}$ and the values of stress exponent n is taken as 5.

The symbols $M(r)$ and σ_o (r) are known as creep parameters and can be obtained from following equations by substituting the values of particle size P, particle content $V(r)$ and operating temperature T at the corresponding locations.

$$M(r) = 0.02876 - \frac{0.00879}{P} - \frac{14.02666}{T} + \frac{0.032236}{V(r)} \tag{6}$$

$$\sigma_o(r) = -0.084P - 0.0232T + 1.1853V(r) + 22.2 \tag{7}$$

In a FG cylinder, particle content varies along with radius. Therefore, both the creep parameters $M(r)$ and σ_o (r) will also vary along the radius of the composite cylinder. In the present study, the particle size (P) is assumed as 1.7 μm while the temperature (T) is assumed as 350°C. Therefore, for a given FG cylinder with known particle size and temperature both the creep parameters will be functions of radius. The values of $M(r)$ and $\sigma_o(r)$ at any radius (r) could be estimated respectively from (6) and (7) by substituting the values of particle size P, particle content $V(r)$ and operating temperature T at the corresponding locations.

IV. MATHEMATICAL ANALYSIS

Consider a long, closed end, thick-walled, hollow cylinder made of functionally graded Al-SiCp composite. The inner and outer radii of cylinder are respectively a and b and the cylinder is subjected to internal pressure p. The coordinates axes r, θ and z are taken respectively along the radial, tangential and axial directions of the cylinder. The present analysis is based on the following assumptions;

i. Material of the cylinder is locally isotropic and stresses at any point in the cylinder remain constant with time.

ii. Elastic deformations are small, therefore, neglected as compared to creep deformations.

The basic strain rate equations are,

$$\dot{\varepsilon}_r = \frac{d\,\dot{\mu}}{d\,r} \tag{8}$$

$$\dot{\varepsilon}_\theta = \frac{\dot{\mu}}{r} \tag{9}$$

where $\dot{\mu} = \frac{d\mu}{dt}$ is the radial displacement rate and $\dot{\mu}$ is the radial displacement.

where $\dot{\varepsilon}_r$ and $\dot{\varepsilon}_\theta$ are radial and tangential strain rates.

Eliminating, $\dot{\mu}$ from (8) and (9), the basic compatibility equation is obtained as,

$$\frac{rd\dot{\varepsilon}_\theta}{dr} = \dot{\varepsilon}_r - \dot{\varepsilon}_\theta \tag{10}$$

The cylinder is subjected to following boundary conditions,

At inner radius; $r=a$; Radial stress, $\sigma_r = -p$ (11)

At outer radius; $r=b$; Radial stress, $\sigma_r = 0$ (12)

The equilibrium equation of thick cylinder [8] can be written as,

$$\sigma_\theta - \sigma_r = r\frac{d\sigma_r}{dr} \tag{13}$$

assuming that the volume of cylinder does not change during entire loading history. Therefore,

$$\dot{\varepsilon}_r + \dot{\varepsilon}_\theta + \dot{\varepsilon}_z = 0 \tag{14}$$

The basic constitutive equations of creep and [8] are given below,

$$\dot{\varepsilon}_r = \frac{\dot{\varepsilon}_e}{2\sigma_e}\left[2\sigma_r - \sigma_\theta - \sigma_z\right] \tag{15}$$

$$\dot{\varepsilon}_\theta = \frac{\dot{\varepsilon}_e}{2\sigma_e}\left[2\sigma_\theta - \sigma_z - \sigma_r\right] \tag{16}$$

$$\dot{\varepsilon}_z = \frac{\dot{\varepsilon}_e}{2\sigma_e}\left[2\sigma_z - \sigma_r - \sigma_\theta\right] \tag{17}$$

where σ_e is the effective stress and $\dot{\varepsilon}_e$ is the effective creep rate invariant.

The von Mises [8] effective stress invariant σ_e is given as below,

$$\sigma_e = \frac{1}{\sqrt{2}}\left[(\sigma_\theta - \sigma_r)^2 + (\sigma_r - \sigma_z)^2 + (\sigma_z - \sigma_\theta)^2\right]^{1/2} \tag{18}$$

The plane strain condition is assumed *i.e.* strain rate along axis of cylinder is zero in the present work, therefore,

$$\dot{\varepsilon}_z = 0 \qquad (19)$$

From (8), (9), (14), (19) displacement rate is,

$$\dot{\mu} = \frac{C}{r} \qquad (20)$$

where 'C' is the constant of integration.
Substituting (20) in (8), we get,

$$\dot{\varepsilon}_r = -\frac{C}{r^2} \qquad (21)$$

By substituting (20) in (9), we obtain,

$$\dot{\varepsilon}_\theta = \frac{C}{r^2} \qquad (22)$$

Also from (17) and (19), we have

$$\sigma_z = \frac{\sigma_r + \sigma_\theta}{2} \qquad (23)$$

By using (23) in (18), the effective stress invariant (σ_e) is given by,

$$\sigma_e = \frac{\sqrt{3}}{2}(\sigma_\theta - \sigma_r) \qquad (24)$$

Substituting the values of $(\dot{\varepsilon}_r)$ and (σ_z) from (21) and (23) in (15), we obtain,

$$(\sigma_r - \sigma_\theta) = -\frac{4}{3} \cdot \frac{\sigma_e}{\dot{\varepsilon}_e} \cdot \frac{C}{r^2} \qquad (25)$$

Substituting the values of (σ_e) and $(\dot{\varepsilon}_e)$ from (24) and (5) in (25), we obtain,

$$(\sigma_r - \sigma_\theta) = \frac{T(r)}{r^{2/n}} + P(r) \qquad (26)$$

where,

$$T(r) = \left[\frac{4}{3}\right]^{\frac{n+1}{2n}} \cdot \left[\frac{-C^{1/n}}{M(r)}\right]$$

$$P(r) = \left[\frac{4}{3}\right]^{1/2} \cdot \sigma_0(r)$$

Solving (13) and (26) and integrating from limit a to r, we get,

$$\sigma_r = -\int_a^r \frac{T(r)}{r^{\frac{n+2}{n}}} . dr - \int_a^r \frac{P(r)}{r} . dr + C_l \qquad (27)$$

where C_l is another constant of integration that can be evaluated by applying boundary conditions given by (11) in (27)

Therefore, (27) becomes,

$$\sigma_r = -\int_a^r \frac{T(r)}{r^{\frac{n+2}{n}}} . dr - \int_a^r \frac{P(r)}{r} . dr - p \qquad (28)$$

By applying another boundary condition given by (12) in (27), the constant 'C' appearing in equation of $T(r)$ can also be estimated.

Using, (28) into (26), tangential stress can be evaluated as below,

$$\sigma_\theta = -\int_a^r \frac{T(r)}{r^{\frac{n+2}{n}}} . dr - \int_a^r \frac{P(r)}{r} . dr - \frac{T(r)}{r^{\frac{2}{n}}} - P(r) - p \qquad (29)$$

Putting, (29) and (28) in (23), axial stress can be evaluated

$$\sigma_z = -\int_a^r \frac{T(r)}{r^{\frac{n+2}{n}}} . dr - \int_a^r \frac{P(r)}{r} . dr - \frac{T(r)}{2r^{\frac{2}{n}}} - \frac{P(r)}{2} - p \qquad (30)$$

Now, substituting the values of (28), (29) and (30) in (15), (16) and (17) to obtain the strain rates in radial, tangential and axial directions respectively.

V. RESULTS AND DISCUSSIONS

On the basis of analysis presented in previous section, numerical calculations have been carried out to obtain creep stresses and strain rates in different composite cylinders (Uniform composite cylinder (UCC), Functionally graded linear cylinder (FGLC), and Functionally graded non-linear cylinder (FGNLC), as mentioned below in Table I.

TABLE I
DESCRIPTION OF CYLINDERS IN PRESENT STUDY

Type of Cylinder	Reinforcement Content (vol %)		
	V_{max}	V_{min}	V_{avg}
Uniform Composite Cylinder (UCC)	20	20	20
Functionally Graded Linear Cylinder (FGLC)	30	12	20
Functionally Graded Non-Linear Cylinder (FGNLC)	30	12	20

A. Validation

Before discussing the results obtained in the present study, it is necessary to check the accuracy of analysis carried out. To accomplish this task, following present analysis, the tangential strain rates have been computed for a cylinder made of copper, for which the results are reported in the literature (Johnson et al. [9]). The dimensions of the cylinder, operating pressure and temperature, and the values of creep parameters

used for the purpose of validation are summarized in Table II. The tangential strain rates thus obtained have been compared with those reported by Johnson et al. [9] and a good agreement is observed in Fig. 1, therefore verifying the accuracy of the analysis presented and the software developed in the current study.
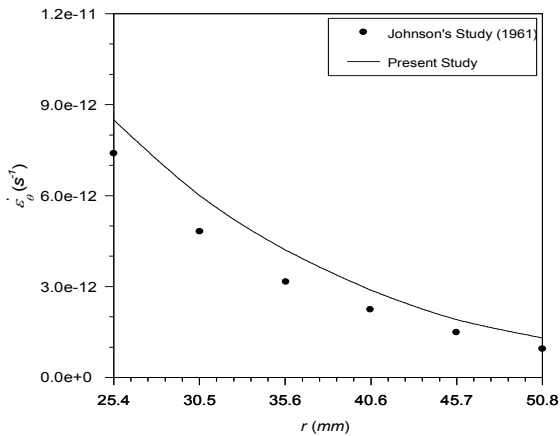

Fig. 1 Comparison of tangential strain rates

TABLE II
DATA USED FOR VALIDATION

Cylinder Material : Copper
Cylinder dimensions: $a = 25.4\ mm$, $b = 50.8\ mm$.
Internal Pressure = 85.25 MPa,
External Pressure = 0
Operating Temperature = 250 ^{o}C
Creep parameters estimated: $M = 3.271 \times 10^{-4} s^{-1/5}/MPa$,
$\sigma_o = 11.32 MPa$

B. Variation of Creep Parameters

The variation of reinforcement (SiCp) in the different cylinders (Table I) taken in the study has been plotted in Fig. 2. The content of SiCp reduces linearly from the inner to outer radius in FGL cylinder while in FGNL cylinder the reinforcement content reduces non-linearly from inner to outer radius but in uniform composite cylinder the reinforcement content remains constant (20 *vol%*) over the entire radius.
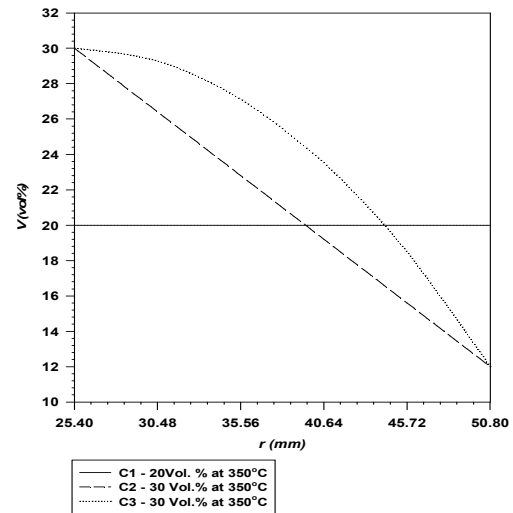

Fig. 2 Distribution of reinforcement

In order to study the effect of particle gradient, on the distribution of creep parameters in the uniform composite cylinder (UCC), functionally graded cylinder (FGLC) and functionally graded non-linear cylinder (FGNLC), the creep parameters has been determined by procedure outlined in Section III and variation is shown in Figs. 3, 4.
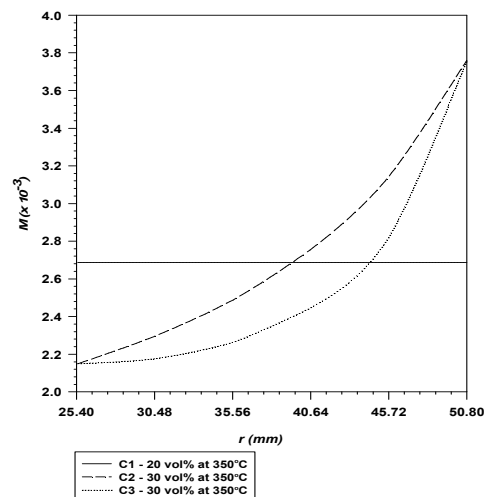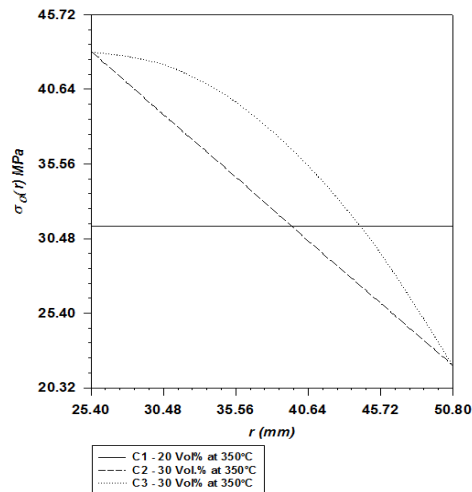

Fig. 3 Distribution of Creep Parameters *M(r)*

Fig. 4 Distribution of Creep Parameters $\sigma_o(r)$

The creep parameter ($M(r)$ and $\sigma_o(r)$) obtained in uniform composite cylinder remains constant because of the same amount of SiCp (20$vol\%$) and uniform temperature ($T = 350^oC$). The creep parameter $M(r)$ increases parabolically on moving from inner radius to outer radius in the FG cylinders (FGLC and FGNLC) but the variation of $M(r)$ in FGNL cylinder is more steeperas compared to FGL cylinder. The increase observed in $M(r)$ for FG cylinders may be due to decrease in particle content $V(r)$ as one move towards the outer radius, Fig. 2. Further, the effect of creep parameters ($M(r)$ and $\sigma_o(r)$) for FG cylinders are entirely opposite to each other as shown in Figs. 3, 4. The threshold stress, $\sigma_o(r)$ shown in Fig. 4 decreases linearly on moving from the inner to outer radius in FGL cylinder but in FGNLC cylinder the creep parameter $\sigma_o(r)$ decreases parabolically on moving from the inner radius to outer radius. The decrease in creep parameter $\sigma_o(r)$ of FGNL cylinder is very slow as compared to FGL cylinder. The decrease observed in $\sigma_o(r)$ of FG cylinders (FGL and FGNL) is due to decrease in particle content $V(r)$ as one move towards from the inner radius to outer radius. The magnitude of threshold stress is large in locations having more amounts of particles as compared to those having lower particle content Pandey et al. [7].

C. Creep Stresses

To study the effect of the particle gradient on steady state creep behavior of uniform composite cylinder and FG cylinders (FGL and FGNL), the steady state stresses have been determined by procedure outlined in Section IV, for three different composite cylinders as mentioned in Table I, and are also plotted in Figs. 5-8. The cylinder taken for investigation in the present work is having same dimensions as that of cylinder used by Johnson et al. [9] in their work.

The radial stress, Fig. 5 remains compressive (negative) throughout the cylinder, with maximum value at the inner radius (85.25 MPa) and zero at the outer radius, due to imposed boundary conditions given by (11) and (12). The compressive value of radial stress decreases almost parabolically throughout all the three composite cylinders (UCC, FGLC and FGNLC). However, the presence of particle gradient leads to reduction in the magnitude of radial stress over the entire radial distance. The FGNL cylinder has averaging effect on the radial stress as compared to UCC and FGNLC.
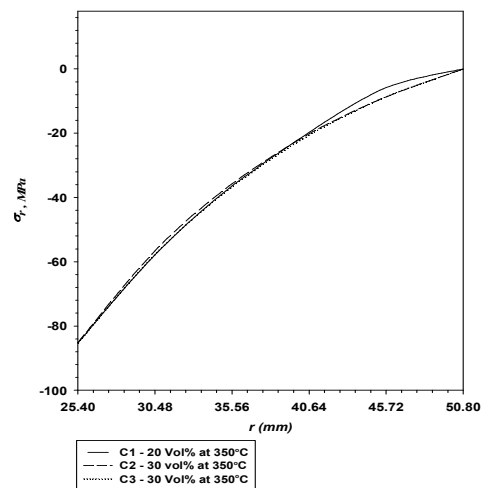

Fig. 5 Distribution of radial stress

The tangential stress shown in Fig. 6 remains tensile throughout in all different composite cylinders and is observed to increase parabolically from inner radius to radius of 45.72 mm but after that it decreases slightly near outer radius for uniform composite cylinder. By incorporating more amounts of silicon carbide particles near the inner radius, as in FGL cylinder, the tangential stress significantly increases by 23 MPa near the inner radius but decreases by 32.53 MPa near outer radius as compared to uniform composite cylinder. The region having relatively more particle offers higher stress compared to the region containing lesser amount of particle. The similar observation had also been reported by Pandey et al. [7] in their experimental investigation of Al-SiC composites. When the FGNL cylinder is subjected to particle gradient, the tangential stress is having averaging effect and its value is in-between the values obtained for composite cylinders (UCC and FGLC). Further, the maxima shift towards the middle region of cylinder.

The axial stress in all the three composite cylinders (UCC, FGLC and FGNLC) changes its nature from compressive (negative) near inner radius and it becomes tensile (positive) near outer radius as shown in Fig. 7. The axial stress in uniform composite cylinder C1 increases parabolically from inner radius to radius of 45.72 mm and then decreases near outer radius. Further, the value of axial stress in FGL cylinder is less compressive as compared to composite cylinders (UCC and FGNLC) but decreases near the outer radius by 16.27 MPa as compared to uniform composite cylinder. The axial

stress near inner radius in FGNL cylinder is less compressive than uniform composite cylinder but more compressive than FGL cylinder. The axial stress in FGNL cylinder is having averaging effect and its value is in-between the values obtained for cylinders (UCC and FGLC).
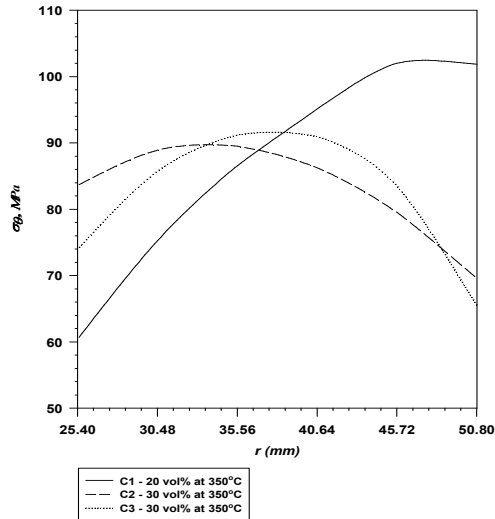

Fig. 6 Distribution of tangential stress

The distribution of von-Mises effective stress is plotted in Fig. 8. The effective stress remains tensile throughout in all the cylinders. Further, the magnitude of effective stress decreases for the entire radial distance in all the three composite cylinders. The effective stress in uniform composite cylinder reduces parabolically throughout the entire radius. By incorporating more amounts of silicon carbide particles near the inner radius, the effective stress in functionally graded linear cylinder increases by 20 *MPa*, near the inner radius and decrease by 28 *MPa*, near the outer radius as compared to uniform composite cylinder. When the FGNL cylinder is subjected to particle gradient, the effective stress has averaging effect and its value lies in between composite cylinders (UCC and FGLC). The magnitude of effective stress is large in locations having more amounts of particles as compared to those having low particle content Pandey et al. [7].
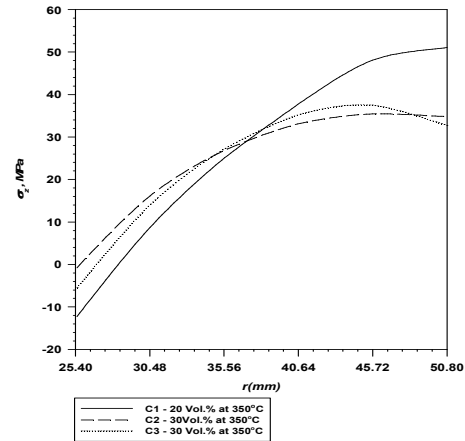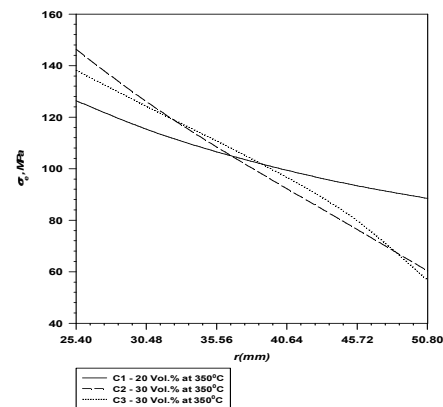

Fig. 7 Distribution of axial stress

Fig. 8 Distribution of effective stress

VI. CONCLUSIONS

The study undertaken has led to the following conclusions;

1. The nature of radial stress is compressive in the composite Al-SiCp cylinders. The compressive value of radial stress decreases parabolically throughout the three cylinders.
2. The tangential stress remains tensile throughout and is observed to increase parabolically from inner radius to outer radius of composite cylinders.
3. The tangential stress significantly increases near inner radius but decreases near outer radius due to presence of particle gradient (linear or non-linear).
4. The axial stress in all composite cylinders changes its nature from compressive (negative) at the inner radius and it becomes tensile (positive) at the outer radius.
5. The effective stress remains tensile throughout in all composite cylinders. Further, the magnitude of effective stress decreases for the entire radial distance in all the three composite cylinders (UCC, FGLC and FGNLC by incorporating particle gradient.

REFERENCES

[1] Noda, N., Nakai, and S., Tsuji, T. "Thermal stresses in functionally graded materials of particle- reinforced composite", *JSME Int J Series A, v*ol. 41(2), pp. 178-184, 1998.

[2] Fukui, Y. and Yamanaka, N. "Elastic Analysis for Thick-Walled Tubes of Functionally Graded Material Subjected to Internal Pressure", *JSME Int J Series I,* vol. 35(4), pp. 379-385, 1992.

[3] Chen, J.J., Tu, S.T., Xuan, F.Z., and Wang, Z.D. "Creep analysis for a functionally graded cylinder subjected to internal and external pressure", *The J Strain Analysis for Engng Design*, vol. 42(2), pp. 69-77, 2007.

[4] You, L.H., Ou, H., and Zheng, Z.Y. "Creep deformations and stresses in thick-walled cylindrical vessels of functionally graded materials subject to internal pressure", *Composite Structure*, vol. 78, pp. 285-291, 2007.

[5] Abrinia, K., Naee, H., Sadeghi, F., and Djavanroodi, F.."New analysis for the FGM thick cylinders under combined pressure and temperature loading", *American J of Applied Sc,* vol. 5 (7), pp. 852-859, 2008.

[6] Tjong, S.C., and Ma, Z.Y. "Microstructural and mechanical characteristics of in situ metal matrix composites", *Mater SciEngng*, vol. R29 (3-4), pp. 49-113, 2000.

[7] Pandey, A.B., Mishra, and R.S., Mahajan, "Y.R. Steady state creep behavior of silicon carbide particulate reinforced aluminium composites", *ActaMetall Mater*, vol. 40(8), pp. 2045-2052, 1992.

[8] Bhatnagar, N.S., and Gupta, S.K. "Analysis of thick-walled orthotropic cylinder in the theory of creep", *J. of Physical Soc. of Japan*, vol. 27(6), pp. 1655–1662, 1969.

[9] Johnson, A.E., Henderson, J., and Khan, B. "Behavior of metallic thick-walled cylindrical vessels or tubes subjected to high internal or external pressures at elevated temperatures", *ProcInstnMechEngrs*, vol. 175(25), pp. 1043-1069, 1961.